Spectral Correlation Density Estimation via Minimum Variance Distortion-less Response Filterbanks

Horacio Sanson and Mitsuji Matsumoto

1 Summary

Previous work in Spectral Correlation Density (SCD) estimation of cyclostationary signals has been based on the Weighted Overlapped Segment Averaging (WOSA) estimator that is known to have low resolution and high frequency leakage. In this paper we address the estimation of the SCD using the high resolution Minimum Variance Distortion-less Response (MVDR) estimator. Using the Matched Filterbank (MAFI) approach to spectral estimation we derive SCD estimators based on the classic WOSA and MVDR. The MAFI approach provides a common base that allows direct comparison between the SCD estimators and gives better insight of the relation between them. Numerical examples are presented to validate the derived estimators and to quantitatively evaluate their performance in terms of cycle frequency resolution, variance and bias of the SCD estimates.

2 Introduction

In several engineering and science fields most signals are generated by means of periodic processes (i.e. modulation) and as a consequence the generated signals exhibit (second order) moments that are periodic in time. These signals are better modeled as cyclostationary and can be characterized by cyclic descriptors like the *cyclic auto-correlation* and *spectral correlation density* [2].

These cyclic descriptors are fundamental tools from where more complex cyclic descriptors can be obtained like the *cyclic magnitude* and *cyclic phase*, the *cyclic coherence spectrum* and the *cyclic Wigner-Ville* spectrum that have a rich set of practical applications in communication systems, mechanical vibration analysis, meteorology, economics, hydrology and acoustics [1, 5, 6, 7, 8, 20].

For most applications it is often more convenient and natural to analyze the structure of cyclostationary signals in the frequency domain. Therefore, it is of practical interest to estimate the spectral correlation density (SCD) from samples of the observed signal.

Most of the proposed SCD estimators in the literature are based on WOSA [9] that is well known to have poor resolution properties and large spectral leakage [1] [5]. These limitations are especially troublesome when we deal with short length observations of the signal that is a common occurrence in practical systems. The Minimum Variance Distortion-less Response (MVDR) [3, 11] has gained attention in the last decade in array processing and spectral estimation due to its higher resolution capabilities even with short length observations. In this work we argue that SCD estimation can also benefit from these high resolution properties and evaluate MVDR as a good alternative for SCD estimation.

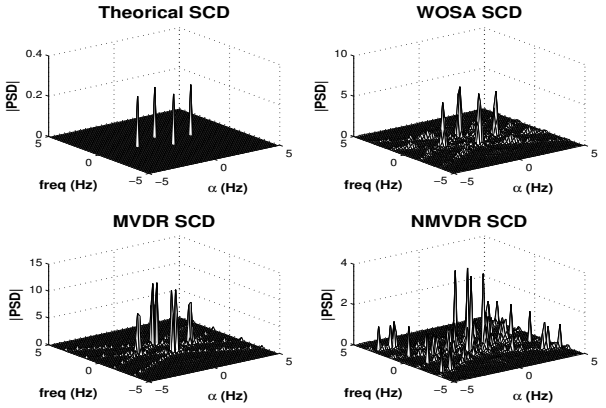

Fig. 1 Theoretical and estimated SCD.

For evaluation purposes we derive three estimators, two based on MVDR and one based on WOSA, using a Matched Filterbank (MAFI) approach [21, 16]. The MAFI approach provides a common base where each method only differs in the filters design and their bandwidth estimate. This allows direct comparison between methods and simplifies their implementation.

In the next section we present a short review of the SCD and present a simple example of cyclostationary signal that is used later to validate the derived SCD estimators. We also formulate the SCD estimation problem as a joint spectrum estimation problem (i.e. cross spectrum) using Cyclic Demodulates. In section 4 following the MAFI approach, we derive cross spectrum estimators based on MVDR and WOSA and present how these estimators can be used to estimate the SCD. In section 5 we evaluate numerically the statistical properties of these estimators in terms of cycle frequency

resolution, bias and variance and finally in 6 we present some discussion on the numerical results and future research work.

3 The Spectral Correlation Density

A zero mean stochastic process $x(n)$ is cyclostationary (in the wide sense) if the auto correlation function given by

$$R_x(n,\tau) = E\{x(n+\tau/2)x^*(n-\tau/2)\} \quad (1)$$

is periodic in time with an integer period N:

$$R_x(n,\tau) = R_x(n+lN,\tau); \forall n, l \in Z \quad (2)$$

Since the auto-correlation $R_x(n,\tau)$ is periodic it accepts Fourier Series expansion and can be written as:

$$R_x(n,\tau) = \sum_{\alpha} R_x^{\alpha}(\tau)e^{-\imath\alpha n} \quad (3)$$

where the Fourier coefficients:

$$R_x^{\alpha}(\tau) = \lim_{N\to\infty} \frac{1}{N} \sum_{n=0}^{N-1} R_x(n,\tau)e^{\imath\alpha n} \quad (4)$$

are the *cyclic auto correlations* and $\alpha = \{2\pi k/N\}_{k=-N}^{N}$ are the *cyclic frequencies*. Note that for $\alpha = 0$ the cyclic correlation $R_x^{\alpha}(\tau)$ reduces to the conventional auto correlation. As with conventional spectral analysis it can be shown that the Fourier Transform of these lag-dependent coefficients give raise to the *spectral correlation density* (SCD)[5]:

$$S^{\alpha}(\omega) = \sum_{\tau=-\infty}^{+\infty} R_x^{\alpha}(\tau)e^{-\imath\omega\tau} \quad (5)$$

The above equation $S^{\alpha}(\omega)$ displays the power distribution of the signal with respect to both the spectral frequency ω and the cycle frequency α. In this respect the spectral correlation density contains an additional dimension related to the non stationary features of the signal.

3.1 Spectral Correlation Properties

We know from classic spectral estimation theory that the spectrum of a periodic signal with period N is also a periodic sequence with period N. Thus the support region of the spectral correlation in the ω plane is contained between $-\pi \le \omega = 2\pi k/N \le \pi$ with $-N/2 \le k \le N/2$.

Also the spectral correlation density (5) presents the following properties in the bi-frequency plane $\alpha - \omega$ [1]:

$$S^{\alpha}(\omega)^* = S^{-\alpha}(\omega+\alpha) = S^{-\alpha}(-\omega) \quad (6)$$

$$S^{-\alpha}(\omega) = S^{\alpha}(\omega+\alpha)^* = S^{\alpha}(-\omega)^* \quad (7)$$

These symmetry properties in the bifrequency plane added to the periodicity in the ω plane restrict the frequency support of the spectral correlation to the principal quadrant of the bi-frequency plane.

3.2 Example of a Cyclostationary Signal

A simple example of cyclostationary signal is an harmonic sinusoid in additive noise:

$$x(n) = Acos(\omega_c n + \phi) + v(n) \quad (8)$$

where $v(n)$ is assumed real, stationary white noise with zero mean and variance σ_v^2, A is a constant amplitude and ω_c and ϕ are deterministic constants in $(0,\pi)$ and $(-\pi,\pi]$ respectively. Using equation (4) and equation (5) we can derive an expression for the SCD of this model as [6, 8]:

$$S_x^{\alpha}(\omega) = \frac{A^2}{4}\left[\delta(\omega-\omega_c)+\delta(\omega+\omega_c)\right]\delta(\alpha) + \frac{A^2}{4}\left[e^{\imath 2\phi}\delta(\alpha-2\omega_c)+e^{-\imath 2\phi}\delta(\alpha+2\omega_c)\right] + \sigma_v^2\delta(\alpha) \quad (9)$$

For a signal with zero phase the SCD would have two peaks at $(\omega,\alpha) = (\pm\omega_c, 0)$ of amplitude $A^2/4 + \sigma_v^2$ and two peaks at $(\omega,\alpha) = (0, \pm 2\omega_c)$ with amplitude $A^2/4$.

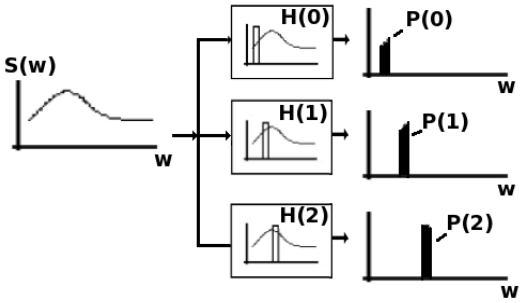

Fig. 2 Filter bank interpretation to spectral density estimation.

3.3 Cyclic Demodulation

To understand this interpretation we simply have to insert the auto correlation function definition given by equation (1) into (4):

$$R_x^{\alpha}(\tau) = E\{x(n+\tau/2)x^*(n-\tau/2)\}e^{-\imath\alpha n} \quad (10)$$

then define $u(n)$ and $v(n)$ such that:

$$u(n) = x(n)e^{-\imath\frac{\alpha}{2}n} \tag{11}$$

$$v(n) = x(n)e^{\imath\frac{\alpha}{2}n} \tag{12}$$

replace them in equation (10) to obtain:

$$R_x^\alpha(\tau) = E\left\{u(n+\tau/2)v^*(n-\tau/2)\right\} \tag{13}$$

The equation above shows that $R_x^\alpha(\tau)$ is the cross correlation of $u(n)$ and $v(n)$, and therefore from equation (5) follows that $S^\alpha(\omega)$ is the cross spectral density of $u(n)$ and $v(n)$. This interpretation suggests that $S^\alpha(\omega)$ can be estimated using any cross PSD estimator such as the WOSA and MVDR.

4 Filter bank PSD estimation

The concept of spectral estimation via filter banks is depicted in figure 2. Basically we have a zero mean signal vector $\mathbf{x_n} = [x(n), x(n-1), \ldots, x(n-Q+1)]^T$ with spectral density $S(\omega)$ and pass it through a bank of narrow band filters $\mathbf{h}_\omega = [h(0), h(1), \ldots, h(Q-1)]^T$ each one steered at a different frequency ω. The output at the filters is given by:

$$y(n) = \sum_{q=0}^{Q-1} h(q)x(n-q) = \mathbf{h}^H\mathbf{x_n} \tag{14}$$

and the output power $P(\omega)$ is:

$$P(\omega) = E\left\{|y(n)|^2\right\} = \mathbf{h}_\omega{}^H\mathbf{R_{xx}}\mathbf{h}_\omega \tag{15}$$

where $\mathbf{R_{xx}}$ is an estimate of the auto correlation matrix of $\mathbf{x_n}$. By measuring the output power $P(\omega)$ at one filter we can estimate the spectral density $S(\omega)$ by the relation [12, 14]:

$$S(\omega) = \frac{P(\omega)}{B_N} = \frac{\mathbf{h}_\omega{}^H\mathbf{R_{xx}}\mathbf{h}_\omega}{B_N} \tag{16}$$

at the frequency the filter is steered and where B_N is an estimate of the effective filter bandwidth.

Based on equation (16) we can then design different $S(\omega)$ estimators by choosing different filters and bandwidth parameters.

4.1 WOSA Method

The simplest filter $\mathbf{h}_{\omega_c}$ we could design is a rectangular window of N samples with amplitude one:

$$\mathbf{h} = [1, 1, \ldots, 1]^T \tag{17}$$

this filter steered at a frequency ω becomes:

$$\mathbf{h}_\omega = \left[1, e^{j\omega}, \ldots, e^{j(N-1)\omega}\right]^T \tag{18}$$

and has constant bandwidth:

$$B_N = \mathbf{h}_\omega{}^H\mathbf{h}_\omega = N \tag{19}$$

Replacing these into equation (16) we get:

$$S(\omega) = \frac{\mathbf{a}_\omega{}^H\mathbf{R_{xx}}\mathbf{a}_\omega}{N} \tag{20}$$

where $\mathbf{a}_\omega$ is known as the steering vector and is defined as:

$$\mathbf{a}_\omega = \left[1, e^{j\omega}, \ldots, e^{j(N-1)\omega}\right]^T \tag{21}$$

Equation (20) is the general *Weighted Overlapped Spectrum Averaging* (WOSA) spectral estimator. In this basic form equation (20) is equivalent to the well known periodogram:

$$S(\omega) = \frac{\mathbf{a}_\omega{}^H\mathbf{x_n}\mathbf{x_n}{}^H\mathbf{a}_\omega}{N} = \frac{1}{N}\left|\mathbf{a}_\omega{}^H\mathbf{x_n}\right|^2 \tag{22}$$

$$= \frac{1}{N}\left|\sum_{n=0}^{N-1} x(n)e^{-jn\omega}\right|^2 = \frac{1}{N}\left|DFT(x(n))\right|^2 \tag{23}$$

By splitting the signal vector $\mathbf{x_n}$ in segments of length Q and averaging the spectral densities of each segment we can obtain the Bartlet (Averaged Periodogram) method:

$$\mathbf{R_{xx}} = \frac{1}{M}\sum_{m=0}^{M-1}\mathbf{x_m}\mathbf{x_m}{}^H \tag{24}$$

where $M = N/Q$ is the number of segments and

$\mathbf{x_m} = [x(mQ), x(mQ-1), \ldots, x(mQ-Q+1)]^T$.

Using this correlation matrix the estimator becomes:

$$S(\omega) = \frac{1}{M}\sum_{m=0}^{M-1}\frac{\mathbf{a}_\omega{}^H\mathbf{x_m}\mathbf{x_m}{}^H\mathbf{a}_\omega}{Q} \tag{25}$$

$$= \frac{1}{M}\sum_{m=0}^{M-1}\left|DFT(x(m))\right|^2/Q \tag{26}$$

We could also apply windows (filter) $\mathbf{R_{xx}}$ and/or overlap the segments; operations that would result in other classic non-parametric methods of spectral estimation. During our numerical examples we won't use any pre windows as they further degrade the already poor resolution of the WOSA method and will always use maximum overlapping of

segments that presents the minimum cycle leakage for the WOSA method [1].

4.2 MVDR Method

The square filter used by WOSA has a *sinc* shaped impulse response $H(\omega_c)$ as shown in figure 3 and as we can see this shape has a direct impact in the estimate of $P(\omega_c)$.

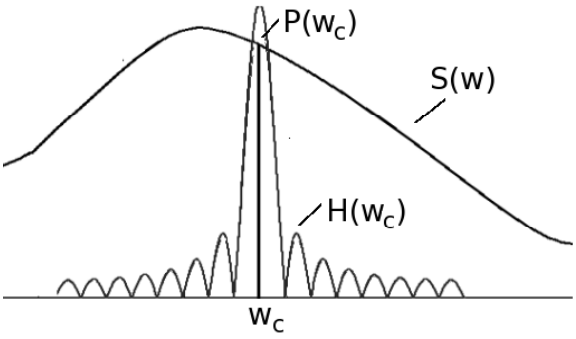

Fig. 3 Spectral density estimation via filtering.

To improve the estimate MVDR implements a narrow band filter with impulse response equal to unity (distortion-less) at the frequency ω_c while reducing as much as possible the power at the other frequency bands (minimum variance) [11].

This filter design is a well known optimization problem where we solve for $\mathbf{h}_{\omega_c}$ by minimizing the power:

$$\mathbf{h}_{\omega_c} = \mathbf{h}_{\omega_c}{}^{H}\mathbf{R}_{\mathbf{xx}}\mathbf{h}_{\omega_c} \tag{27}$$

subject to the constraint $\mathbf{h}_{\omega_c}{}^{H}\mathbf{a} = 1$ where $\mathbf{a}$ is the steering vector defined in (21).

This optimization problem has a known solution given by [3, 11]:

$$\mathbf{h}_{\omega_c} = \frac{\mathbf{R}_{\mathbf{xx}}^{-1}\mathbf{a}}{\mathbf{a}^{\mathbf{H}}\mathbf{R}_{\mathbf{xx}}^{-1}\mathbf{a}} \tag{28}$$

replacing this in (15) gives the PSC (Power Spectrum Capon) estimator:

$$P(\omega_c) = \frac{1}{\mathbf{a}^{\mathbf{H}}\mathbf{R}_{\mathbf{xx}}^{-1}\mathbf{a}} \tag{29}$$

To get $S(\omega_c)$ we must normalize $P(\omega_c)$ by the filter bandwidth B_N as per relation (16). A simple estimate of B_N is given by the reciprocal of the filter length, that is $B_N = 1/Q$, that results in the MVDR estimator [3]:

$$S_{MVDR}(\omega_c) = \frac{Q}{\mathbf{a}^{\mathbf{H}}\mathbf{R}_{\mathbf{xx}}^{-1}\mathbf{a}} \tag{30}$$

Another estimator known as normalized MVDR or NMVDR is obtained by using the relation $B_N = \mathbf{a}^{\mathbf{H}}\mathbf{a}$ that results in [13]:

$$S_{NMVDR}(\omega_c) = \frac{\mathbf{a}^{\mathbf{H}}\mathbf{R}_{\mathbf{xx}}^{-1}\mathbf{a}}{\mathbf{a}^{\mathbf{H}}\mathbf{R}_{\mathbf{xx}}^{-2}\mathbf{a}} \tag{31}$$

We can see from equations (30) and (31) that both MVDR and NMVDR are adaptive filters as they depend on the signal features R_{xx}. This is in contrasts with the rectangular filter used by WOSA that is generic and does not consider the signal to be filtered in its construction.

4.3 Cross Power Spectrum Estimation and SCD Estimation.

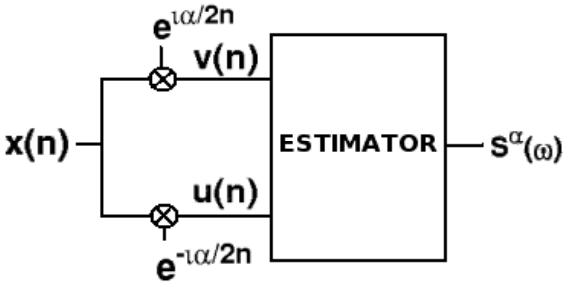

Fig. 4 SCD Estimation via cyclic demodulates Method.

From a filtering point of view the estimation of the cross power spectrum from two data vectors $\mathbf{x_1}$ and $\mathbf{x_2}$ can be based on the design of two narrow band pass filters $\mathbf{h_{x_1}}$ and $\mathbf{h_{x_2}}$ steered at the same frequency ω_c. Therefore the cross power spectrum can be inferred as the cross correlation of the filter outputs at lag zero [14]:

$$P_{x_1x_2}(\omega) = E\left\{\mathbf{y_1}\mathbf{y_2}^{H}\right\} \tag{32}$$

where $\mathbf{y_1}$ and $\mathbf{y_2}$ are the filter outputs given by $\mathbf{h_{x_1}}{}^{H}\mathbf{x_1}$ and $\mathbf{h_{x_2}}{}^{H}\mathbf{x_2}$ respectively. Using (16), (20), (30), (31) and (32) we can easily find:

$$S_{WOSA}(\omega) = \frac{\mathbf{a}_\omega{}^{H}\mathbf{R}_{\mathbf{x_1x_2}}\mathbf{a}_\omega}{Q} \tag{33}$$

$$S_{MVDR}(\omega) = Q\frac{\mathbf{a}_\omega{}^{H}\mathbf{R}_{\mathbf{x_1x_1}}^{-1}\mathbf{R}_{\mathbf{x_1x_2}}\mathbf{R}_{\mathbf{x_2x_2}}^{-1}\mathbf{a}_\omega}{\mathbf{a}_\omega{}^{H}\mathbf{R}_{\mathbf{x_1x_1}}^{-1}\mathbf{a}_\omega\mathbf{a}_\omega{}^{H}\mathbf{R}_{\mathbf{x_2x_2}}^{-1}\mathbf{a}_\omega} \tag{34}$$

$$S_{NMVDR}(\omega) = \frac{\mathbf{a}_\omega{}^{H}\mathbf{R}_{\mathbf{x_1x_1}}^{-1}\mathbf{R}_{\mathbf{x_1x_2}}\mathbf{R}_{\mathbf{x_2x_2}}^{-1}\mathbf{a}_\omega}{\mathbf{a}_\omega{}^{H}\mathbf{R}_{\mathbf{x_1x_1}}^{-1}\mathbf{R}_{\mathbf{x_2x_2}}^{-1}\mathbf{a}_\omega} \tag{35}$$

where $\mathbf{R_{x_1x_1}}$, $\mathbf{R_{x_2x_2}}$, and $\mathbf{R_{x_1x_2}}$ are the Q x M auto correlations and the cross correlation respectively of the signal vectors.

Using these cross spectrum estimators we are now able to obtain an estimate of $S^{\alpha}(\omega)$ using the cyclic demodulation procedure described in section 3.3 and shown in figure 4.

The procedure is as follows: for each cyclic frequency α of interest we shift $x(n)$ by a step size $\pm\alpha/2$ to obtain expressions (11) and (12) and use these frequency shifted versions of $x(n)$ as inputs to any of the cross PSD (33), (34) or (35). The output of this is the estimated $S^{\alpha}(\omega)$ at the respective cyclic frequency α.

5 Numerical Evaluation

In the discussion that follows we present the bias, variance and cyclic resolution properties of the SCD estimators presented in section 4.3 with different segment sizes for WOSA and different filter lengths for MVDR and NMVDR. We will refer to each test case with the method name followed by the segment or filter lengths (i.e. WOSA Q).

For WOSA the values of Q represent segment size and take the values N, $N/2$ and $N/4$ where N is the total number of samples of the signal. As mentioned above WOSA N is the known periodogram used extensively in classic spectral estimation. For MVDR and NMVDR Q represents the filter lengths and has a maximum value of $N/2$ because larger values would cause R_{xx} to be singular (i.e. non invertible) that would result in unstable spectral estimates.

In all simulations we generated 64 samples of the example signal presented in section 3.2 with a signal frequency of $f_c = 1.5Hz$ and sampled at $10Hz$.

To simplify our numerical results we set the amplitude to $A = 1$. Also based on the periodic and symmetric properties of the spectral correlation (section 3.1) we only estimate the first quadrant of $S^{\alpha}(\omega)$ in the bi-frequency plane $\alpha - \omega$ and obtain the other three quadrants using the symmetry properties. This greatly reduces the computation time and memory consumption of our algorithm.

Before we can estimate $S^{\alpha}(\omega)$ using any of our derived estimators (33), (34) or (35) we need to estimate $\mathbf{R_{xx}}$ first.

We have the forward estimate:

$$\hat{R}_F = \frac{1}{N}\sum_{n=0}^{N-1} x(n)x^*(n) \tag{36}$$

or the forward-backward sample estimate:

$$\hat{R}_{FB} = \frac{1}{2}(\hat{R}_F + J\hat{R}_F^T J) \tag{37}$$

where J is the reflection matrix. We prefer to use the forward-backward sample estimate as it is known to have better statistical properties than the forward-only estimate [10, 17].

5.1 Probability of cyclic resolution

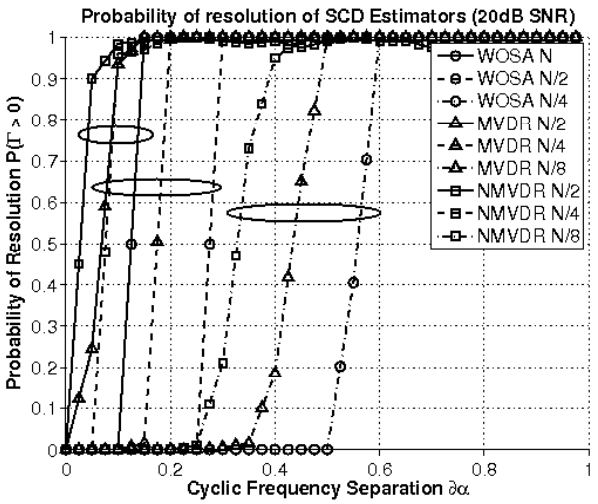

Fig. 5 Probability of resolution.

We are interested in evaluating the probability of resolution of the cyclic frequency α that is characteristic of the SCD.

Although there is no rigorous definition of cyclic frequency resolution we can define a resolution criterion as the frequency separation $\partial\alpha = |\alpha_1 - \alpha_2|$ at which the SCD evaluated at $\alpha_m = (\alpha_1 + \alpha_2)/2$ is equal to the average of the SCDs evaluated at α_1 and α_2 [19, 22]:

$$S^{\alpha_m}(\omega) = \frac{1}{2}\{S^{\alpha_1}(\omega) + S^{\alpha_2}(\omega)\} \tag{38}$$

Using this criterion we can establish a random inequality to define a resolution event:

$$\Gamma(\alpha_1, \alpha_2) = \frac{1}{2}(S^{\alpha_1}(\omega) + S^{\alpha_2}(\omega)) - S^{\alpha_m}(\omega) > 0 \tag{39}$$

Correspondingly we can define the binary *probability of resolution* P_{res} as [22]:

$$P_{res} = P(\Gamma > 0) \tag{40}$$

To evaluate the probability of resolution we generated two signals using the same parameters but with frequencies ω_c and $\omega_c + \partial\alpha$ where $\partial\alpha$ takes values from $0Hz$ to $1Hz$ in steps

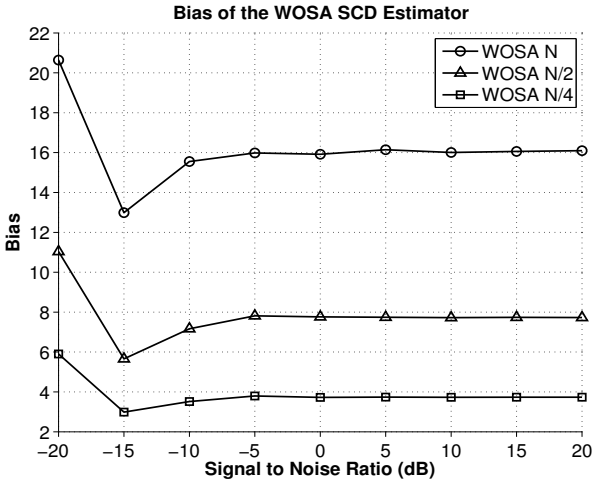

Fig. 6 Bias of the WOSA SCD estimator.

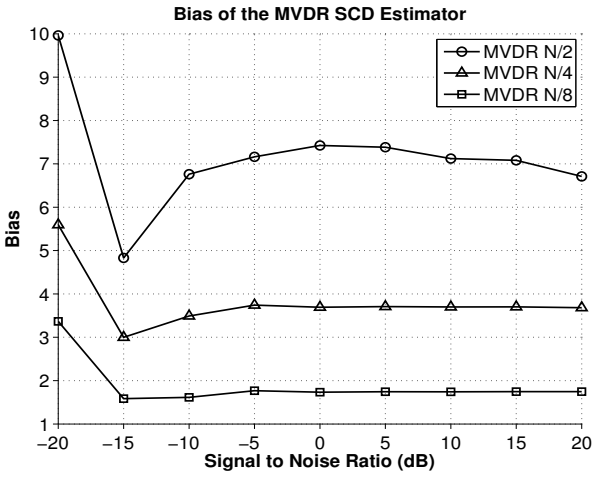

Fig. 7 Bias of the WOSA MVDR estimator.

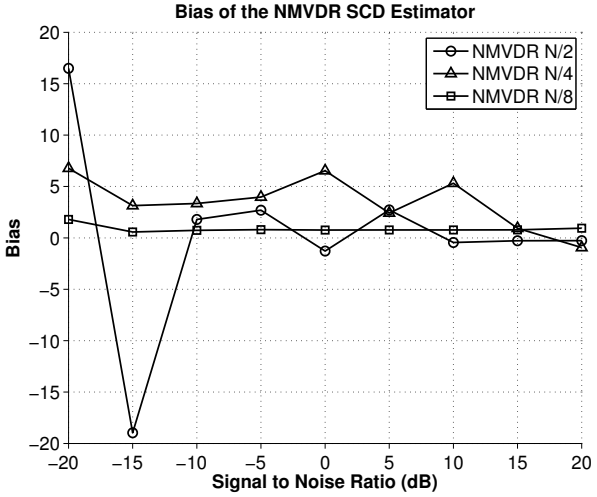

Fig. 8 Bias of the WOSA NMVDR estimator.

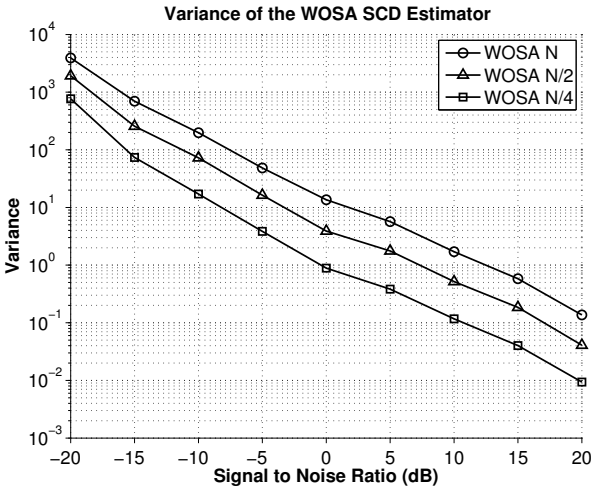

Fig. 9 Variance of the WOSA SCD estimator .

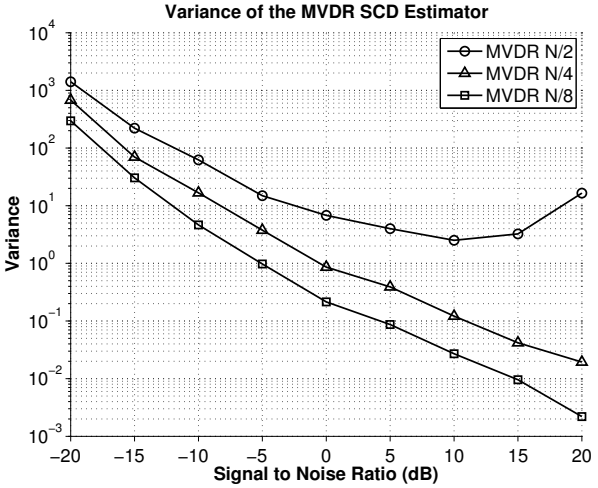

Fig. 10 Variance of the MVDR SCD estimator .

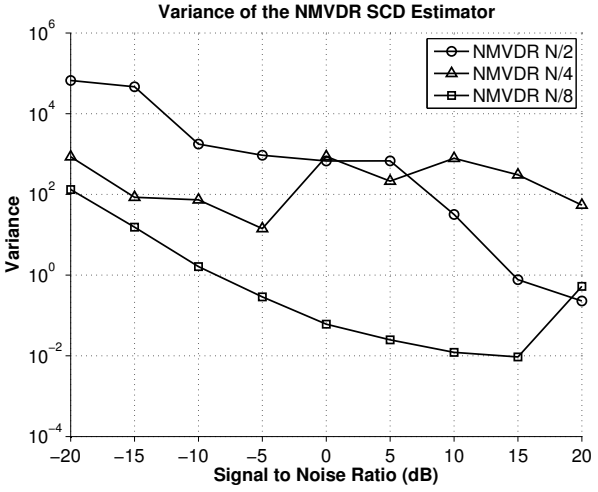

Fig. 11 Variance of the NMVDR SCD estimator.

of $0.05Hz$. This two signals added together result in a SCD similar to those in figure 1 with four additional peaks at:
$(\omega, \alpha) = (\pm\omega_c + \partial\alpha, 0)$
and
$(\omega, \alpha) = (0, \pm 2(\omega_c + \partial\alpha))$.

In figure 5 we plotted the probability of cyclic resolution $P(\Gamma > 0)$ of the two peaks at $(0, \omega_c)$ and $(0, 2(\omega_c + \partial\alpha))$ as a function of the cyclic frequency separation $\partial\alpha$.

As seen in the figure, all test cases present a threshold effect where the probability of resolution is zero until the smaller $\partial\alpha$ resolvable by each test configuration is reached. At this threshold point all methods, except for NMVDR $N/8$, rapidly achieve 100% probability of resolution of the two peaks.

All methods of the same segment/filter size have similar probability of resolution marked by the circular regions in the plot. In all three circular lines NMVDR presents the best resolution followed by MVDR and finally WOSA. As segment/filter length increases all three methods improve in resolution capability but even with no averaging (WOSA N) WOSA lacks behind NMVDR $N/4$ in resolution.

This high resolution property, when compared to WOSA, is one of the praised strengths of the MVDR and NMVDR estimators and as we can see cyclic spectral analysis also benefits from this high resolution property.

5.2 Bias and Variance

To obtain the bias and variance of the SCD estimators we estimated the SCD at the point $(\omega, \alpha) = (0, 2\omega_c)$ over a range of SNR values from $-20dB$ to $+20dB$ using different segment sizes for WOSA and filter lengths for MVDR and NMVDR estimators. For each value of SNR we repeated the experiment over 200 independent trials while accumulating the bias, variance and minimum squared error (MSE) of the spectrum magnitude estimates.

From the bias plots 6, 7 and 8 we can see that all estimators are biased with WOSA N having the largest bias. For segments sizes and filter lengths below $N/4$ we find that MVDR and WOSA estimators presents similar bias while NMVDR goes to both extremes, it has the lowest bias at $N/8$ but quickly increases for larger filter lengths

In the variance plots 9, 10 and 11 we see that WOSA and MVDR, as with the bias, present a similar behavior that improves as the SNR increases and with MVDR slightly better than WOSA. Also as with the bias, NMVDR has the lowest variance at $N/8$ but also presents a quick degradation for larger filter lengths and SNR values.

To make an overall performance comparison between the estimators we plotted their Minimum Square Error (MSE) in Fig. 11. WOSA $N/2$, MVDR $N/2$ and WOSA$N/4$, MVDR $N/4$ present very similar performance as seen also in the bias and variance plots. These performance similarities appear because MVDR can be though as an adaptive version of the WOSA method. To see this it suffices to replace $\mathbf{R}_{\mathbf{x_1x_1}}^{-1}$ and $\mathbf{R}_{\mathbf{x_2x_2}}^{-1}$ in (34) with the identity matrix I and it will reduce to the WOSA estimator (33) [15]. NMVDR has the lowest MSE with short filter length but the performance degrades significantly as larger filters are used. Again we can see a trade-off in performance vs. segment/filter lengths as seen in the probability of resolution but in the opposite direction. Increasing lengths improves resolution but degrades the MSE performance while decreasing lengths improves MSE but reduces resolution.

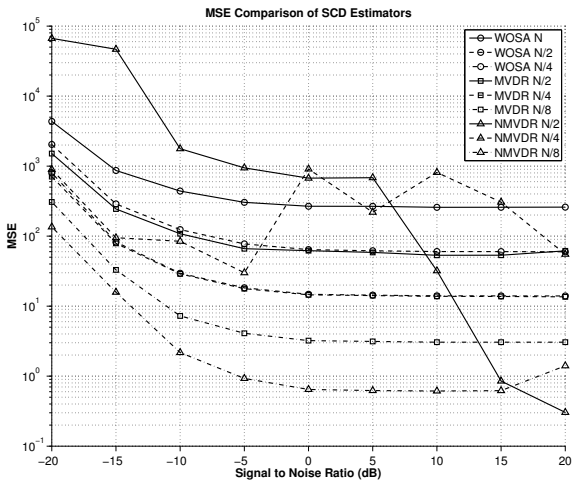

Fig. 12 MSE of SCD Estimators.

6 Conclusions and Future Work

For applications that require to separate very closely spaced frequency components and do not care about the accuracy of the estimated spectrum magnitude the NMVDR would be the best candidate as it presents the best resolution. In most situations where less resolution is tolerable the MVDR method is a better candidate over the classic WOSA method as it has better resolution and comparable bias and variance. In more stringent applications it is possible to use the high resolution of NMVDR to locate the cyclic frequency bin positions and then use MVDR or the less complex WOSA to obtain SCD magnitude at those bin positions only. This way we may get the best SCD estimate by combining the

properties of these estimators at the cost of higher computational cost.

As noted by others [4,18] the high bias and variance presented by the NMVDR is caused by an over estimated bandwidth B_N. We could improve the SCD estimates by selecting a better B_N but care must be taken that such bandwidth values may result in an increased complexity with a little or no improvement on the final spectral density estimate [12].

Our numerical results show that both MVDR and NMVDR exceed in resolution the classic WOSA method and in the case of the MVDR a small improvement in variance and bias. This suggests that MVDR is a better candidate for SCD estimation . Further research will concentrate in efficient implementations of the MVDR and NMVDR methods to reduce the high computational cost mostly due to the matrix inversion.

Finally we must say that these empirical experiments where designed to test the capacity of the estimators to estimate the SCD of a simple cyclostationary signal and for that they are not exhaustive and analytical studies are required to obtain more compete results.

7 Bibliography

[1] J. Antoni. Cyclic spectral analysis in practice. *Mechanical Systems and Signal Processing*, 21:597–630, February 2007.

[2] R. Boyles and W. Gardner. Cycloergodic properties of discrete- parameter nonstationary stochastic processes. *IEEE Transactions on Information Theory*, 29(1):105,114, January 1983.

[3] J. Capon. High-resolution frequency wavenumber spectrum analysis. *Proceedings of the IEEE*, 57(8):1408–1418, April 1969.

[4] Wang Chengyi and Wang Hongyu. Estimation of cyclic spectra using maximum likelihood filters. *Fourth International Conference on Signal Processing Proceedings*, 1:39–42, 1998.

[5] W. Gardner. Measurement of spectral correlation. *IEEE Transactions on Acoustics, Speech, and Signal Processing*, 34(5):1111–1123, October 1986.

[6] W. Gardner. Spectral correlation of modulated signals: Part i–analog modulation. *IEEE Transactions on Communications*, 35(6):584–594, June 1987.

[7] W. Gardner, W. Brown, and Chen Chih-Kang. Spectral correlation of modulated signals: Part ii–digital modulation. *IEEE Transactions on Communications*, 35(6):595–601, June 1987.

[8] Georgios B. Giannakis. *Digital Signal Processing Handbook*, chapter 17. CRC Press, February 1999. Digital Signal Processing Handbook.

[9] G. Heinzel, A. Rudiger, and R. Schilling. Spectrum and spectral density estimation by the discrete fourier transform (dft), including a comprehensive list of window functions and some new flat-top windows. Technical report, Albert Einstein Institut, Teilinstitut Hannover, February 2002.

[10] M. Jansson and P. Stoica. Analysis of forward-only and forward-backward sample covariances. *IEEE Transactions on Acoustics, Speech, and Signal Processing*, 1999.

[11] R. T. Lacoss. Data Adaptive Spectral Analysis Methods. *Geophysics*, 36:661–675, 1971.

[12] M. Lagunas and A. Gasull. An improved maximum likelihood method for power spectral density estimation. *IEEE Transactions on Acoustics, Speech, and Signal Processing*, 32(1):170–173, February 1984.

[13] M. Lagunas and A. Gasull. Measuring true spectral density from ml filters (nmlm and q-nmlm spectral estimates. *IEEE International Conference on Acoustics, Speech, and Signal Processing*, 9:608–611, March 1984.

[14] M. Lagunas, M. Santamaria, A. Gasull, and A. Moreno. Cross spectrum ml estimate. *IEEE International Conference on ICASSP*, 10:77–80, April 1985.

[15] E. G. Larsson, J. Li, and P. Stoica. *High-resolution nonparametric spectral analysis: theory and applications*, chapter 4. High-Resolution Signal Processing. NY: Marcel-Dekker, New York, 2003.

[16] E. G. Larsson, P. Stoica, and J. Li. Spectral estimation via adaptive filterbank methods: a unified analysis and a new algorithm. *Signal Process.*, 82(12):1991–2001, 2002.

[17] H. Li, J. Li, and P. Stoica. Performance analysis of forward-backward matched-filterbank spectral estimators. *IEEE Transactions on Signal Processing*, July 1998.

[18] H. Li, P. Stoica, and J. Li. Capon estimation of covariance sequences, 1998.

[19] L. Marple. Resolution of conventional fourier, autoregressive, and special arma methods of spectrum analysis. *ICASSP '77.*, 2:74–77, May 1977.

[20] Erchin Serpedin, Flaviu Panduru, Ilkay Sari, and Georgios B. Giannakis. Bibliography on cyclostationarity. *Signal Process.*, 85(12):2233–2303, 2005.

[21] P. Stoica, A. Jakobsson, and J. Li. Matched-filter bank interpretation of some spectral estimators. *Signal Processing*, April 1998.

[22] Q.T. Zhang. Probability of resolution of the music algorithm. *Signal Processing, IEEE Transactions on Acoustics, Speech, and Signal Processing, year =*, 43(4):978–987, April 1995.